

Supporting Information

Prussian Blue Analogues with $\text{Na}_2\text{Ni}_x\text{Co}_y\text{Mn}_z\text{Fe}(\text{CN})_6$ -Multimetallic Structures as Positive and Hydrogen Vanadate as Negative Electrodes in Aqueous Na-Ion Batteries for Solar Energy Storage Applications

Pappu Naskar^a, Biplab Biswas^a, Sourav Laha^{b,*} and Anjan Banerjee^{a,*}

^aDepartment of Chemistry, Presidency University-Kolkata, Kolkata-700073, India

^bDepartment of Chemistry, National Institute of Technology Durgapur, Durgapur-713209, India

Calculations of Diffusion Coefficient (D)

The diffusion coefficients (D) of Na ions in the host structures of PBAs are calculated from EIS data by using Eq. S1.[S1]

$$D = 0.5 \times R^2 \times T^2 \times A^{-2} \times n^{-4} \times F^{-4} \times C^{-2} \times \sigma^{-2} \dots\dots\dots (S1)$$

Herein, R = universal gas constant

T = absolute temperature

A = geometrical area of the electrode

n = number of electron transfers per molecule during oxidation and reduction

F = Faraday constant

C = molar concentration of sodium ions (mole/cm³)

σ = Warburg factor, which is connected to the real component of impedance (Z')

The following equation shows the relationship between Z' and σ .

$$Z' = R_s + R_{ct} + \sigma \omega^{-1/2} \dots\dots\dots (S2)$$

Wherein, ω is the frequency in EIS study.

The linear relationship profiles of Z' with $\omega^{-1/2}$ for PBA-1, PBA-2, PBA-3 and HVO are shown in Figure S1 (a-d), respectively. The Warburg factors (σ) are calculated from the slope of the fitted straight line.

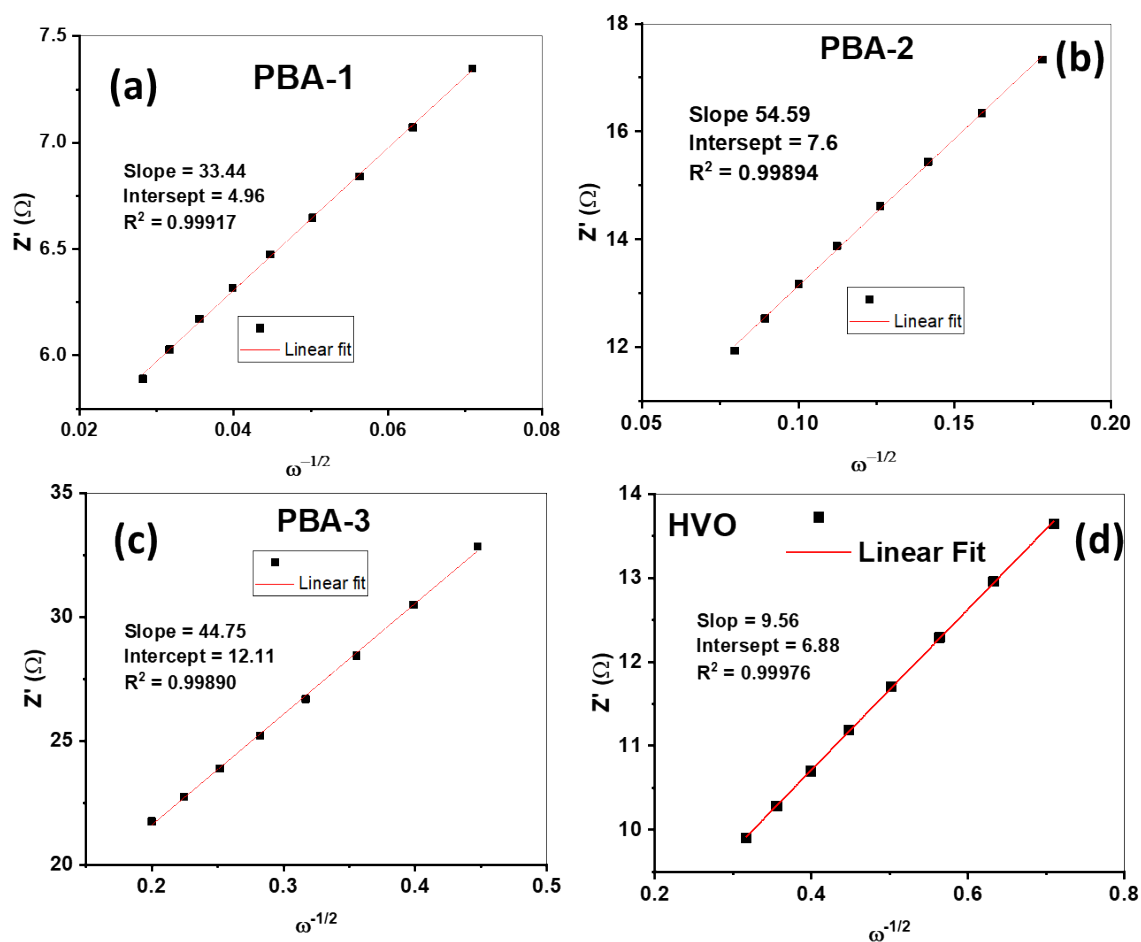


Figure S1: The linear relationship between Z' and $\omega^{-1/2}$ at low-frequency region in EIS (ω = angular frequency) for (a) PBA-1, (b) PBA-2, (c) PBA-3 and (d) HVO.

Table S1. Calculation of Na-ion diffusion coefficient for PBA-1, PBA-2, PBA-3 and HVO

Parameter / Unit	PBA-1	PBA-2	PBA-3	HVO
R (J K ⁻¹ mol ⁻¹)	8.314	8.314	8.314	8.314
T (K)	303	303	303	303
A (cm ²)	1	1	1	1
n	1.66	1.5	1.8	2
F (Coulomb mol ⁻¹)	96485	96485	96485	96485
$\#C$ (mol cm ⁻³)	0.0118	0.012	0.0118	0.001
σ (Ohm s ^{-0.5})	33.44	54.6	44.75	9.56
D (cm ² s ⁻¹)	3.09×10^{-14}	1.68×10^{-14}	1.29×10^{-14}	2.50×10^{-11}

C value is calculated from the crystal structures of the active materials, which are established by Rietveld refinement of PXRD data.

<p>For PBA-1</p> <p>Formula unit per unit cell (Z) = 2</p> <p>Unit cell volume = 558.57 Å³</p> <p>Therefore, 4 Na⁺ ion present in 558.57 Å³</p> <p>Hence, 0.0118 mole Na⁺ ion present in 1 cm⁻³</p>	<p>For PBA-2</p> <p>Formula unit per unit cell (Z) = 2</p> <p>Unit cell volume = 551.96 Å³</p> <p>Therefore, 4 Na⁺ ion present in 551.96 Å³</p> <p>Hence, 0.012 mole Na⁺ ion present in 1 cm⁻³</p>
<p>For PBA-3</p> <p>Formula unit per unit cell (Z) = 2</p> <p>Unit cell volume = 558.39 Å³</p> <p>Therefore, 4 Na⁺ ion present in 558.39 Å³</p> <p>Hence, 0.0118 mole Na⁺ ion present in 1 cm⁻³</p>	<p>For HVO [S2]</p> <p>The HVO structure does not contain Na.</p> <p>Hence, the concentration of Na (mol cm⁻³) in solid structure will be same with the electrolyte's concentration. Herein, C = 0.001 mol cm⁻³</p>

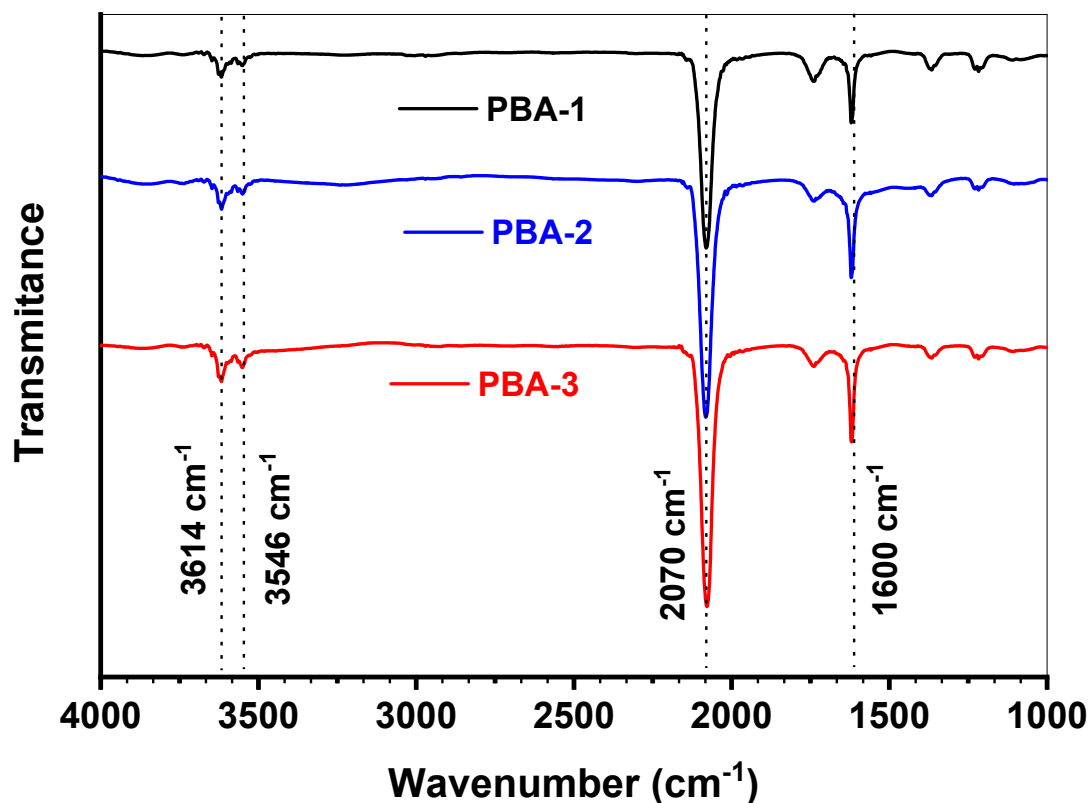


Figure S2: FT-IR spectra of PBA-1, PBA-2 and PBA-3.

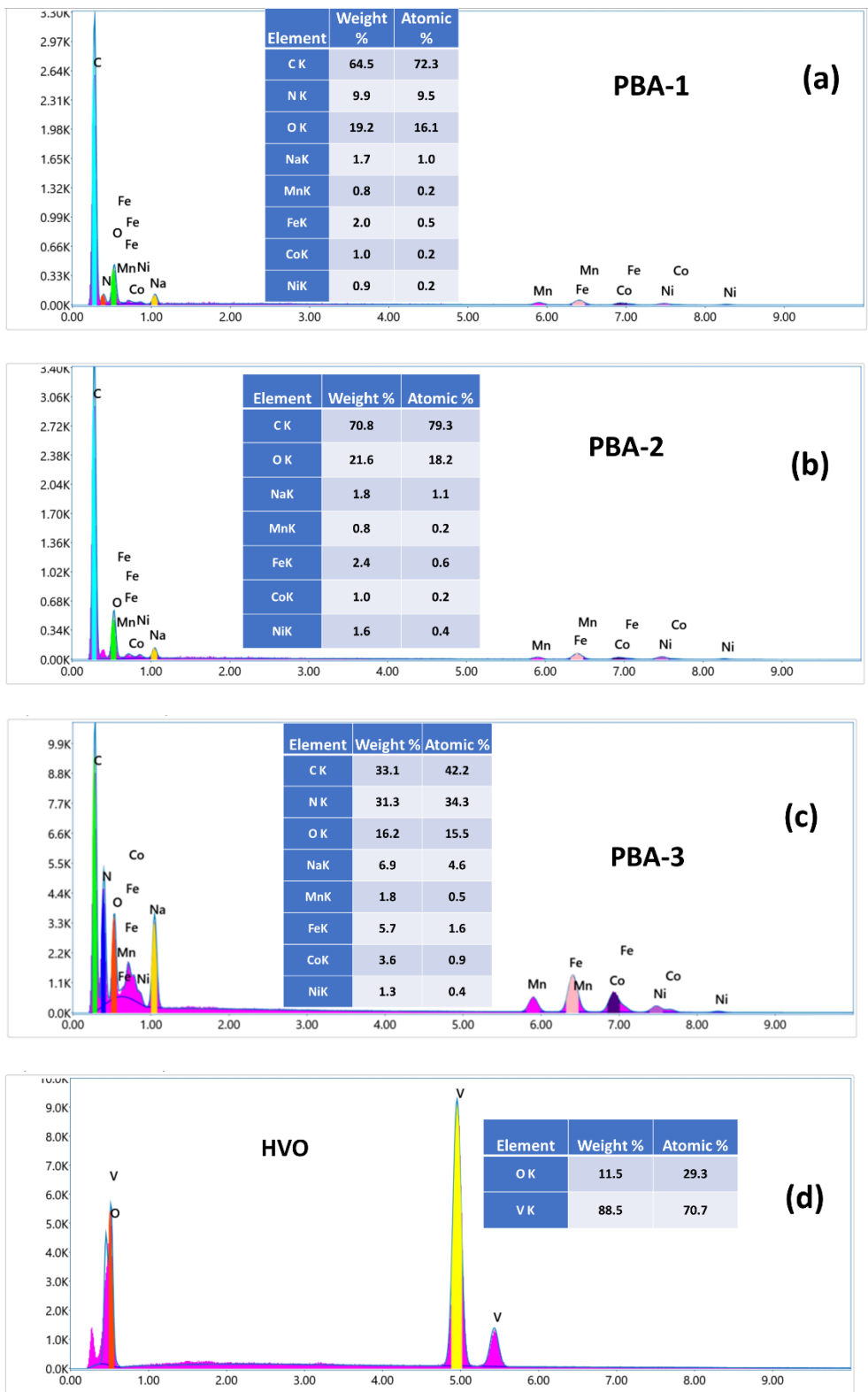


Figure S3: EDX profiles and elemental compositions of (a) PBA-1, (b) PBA-2, (c) PBA-3 and (d) HVO.

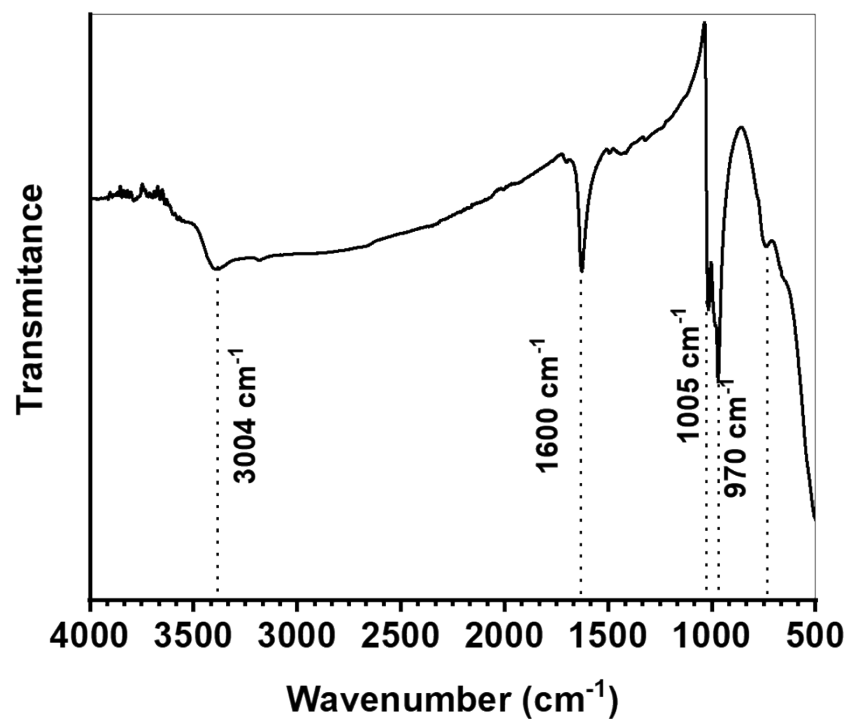


Figure S4: FT-IR spectrum of HVO.

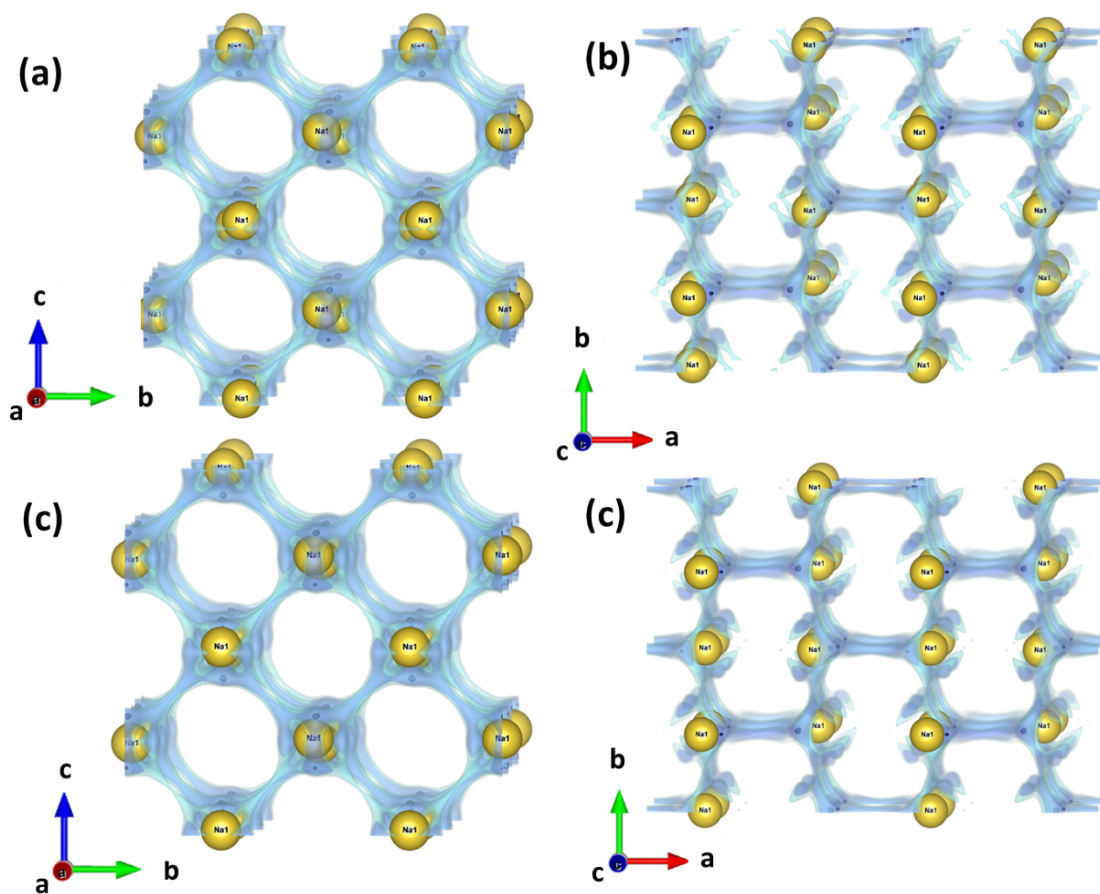


Figure S5: Na-ion diffusion pathways found from BVEL calculations for (a) PBA-2 in b - c plane, (b) PBA-2 in a - b plane, (c) PBA-3 in b - c plane and (d) PBA-3 in a - b plane.

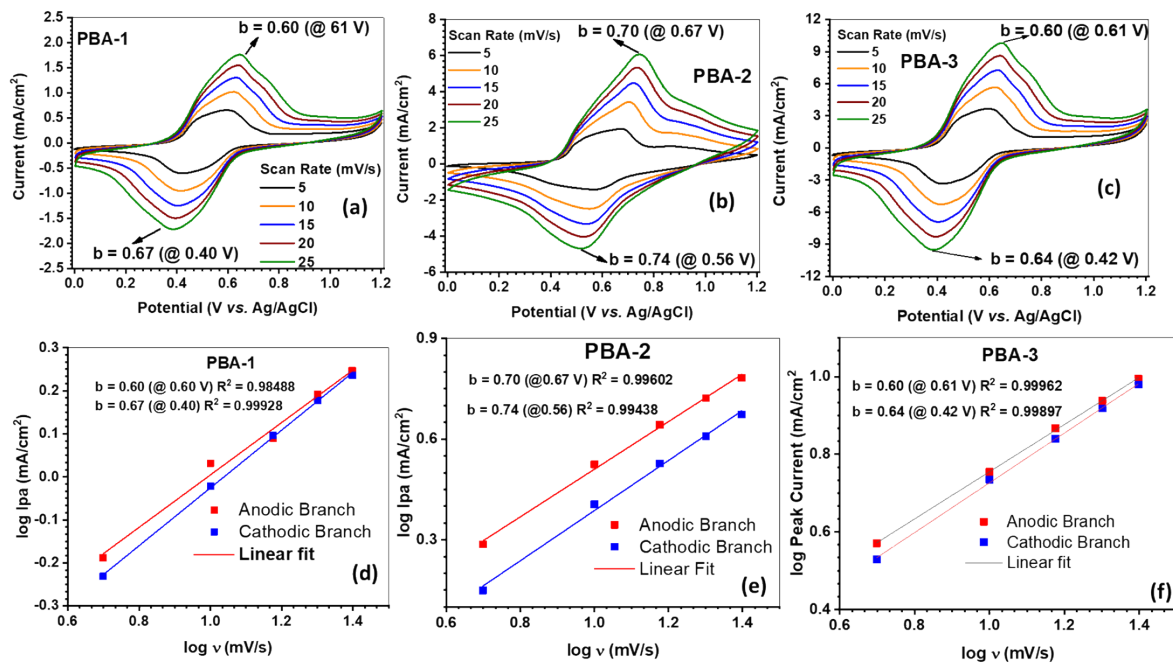


Figure S6: Cyclic voltammograms of (a) PBA-1, (b) PBA-2, (c) PBA-3 within 0-1.2 V vs. Ag/AgCl under the scan rate of 5 to 25 mV s⁻¹; “b” value calculations at the anodic/cathodic peaks for (d) PBA-1, (e) PBA-2, (f) PBA-3.

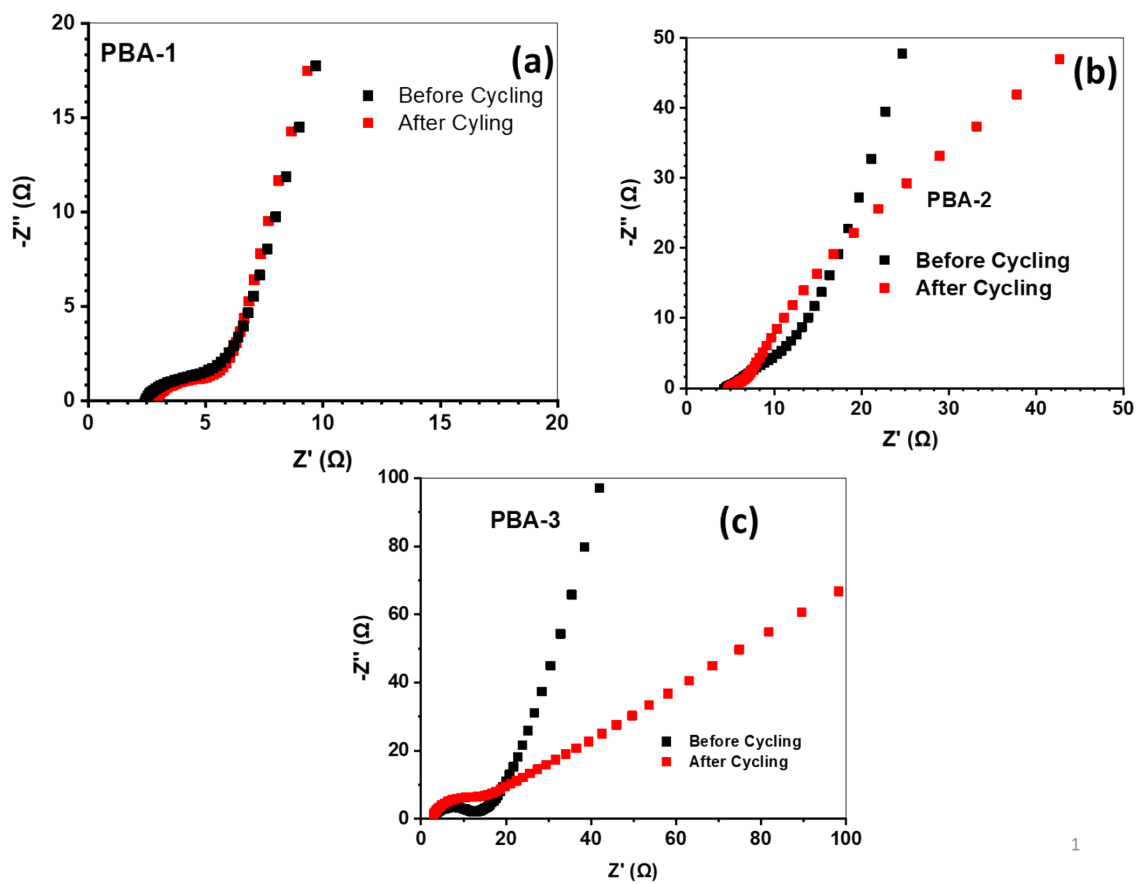


Figure S7: Nyquist plots at before and after cycling experiments for (a) PBA-1, (b) PBA-2 and (c) PBA-3.

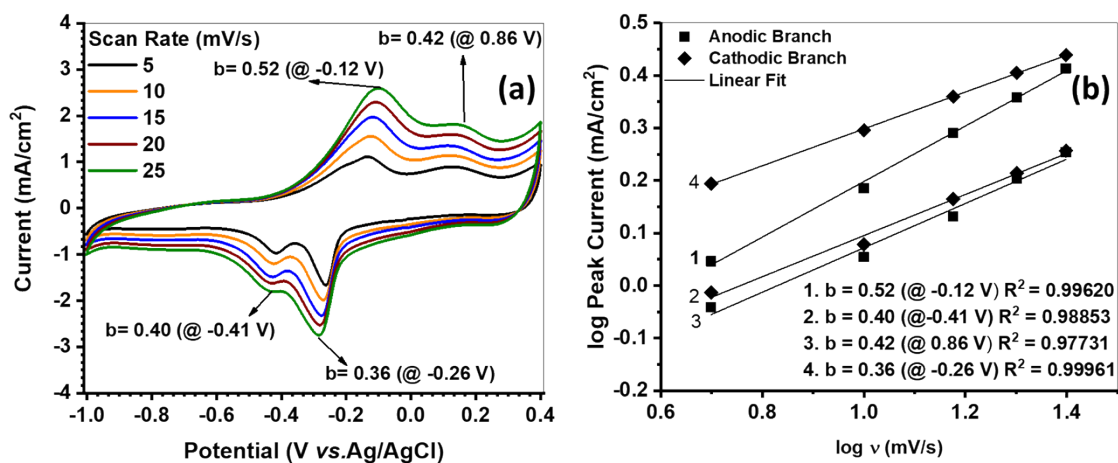


Figure S8: (a) Cyclic voltammograms of HVO within 0.4 to -1.0 V vs. Ag/AgCl under the scan rate of 5 to 25 mV s⁻¹; (b) “b” value calculations at the cathodic/anodic peaks for HVO.

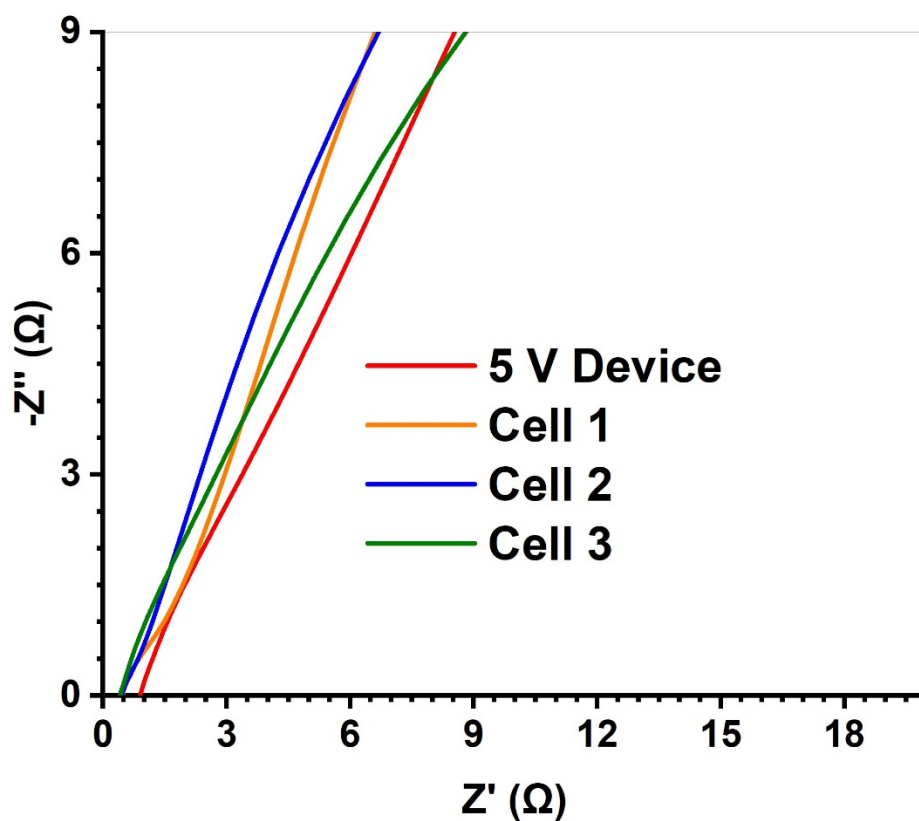


Figure S9: Nyquist plots for 5V device along with three constituent cells at their discharged states.

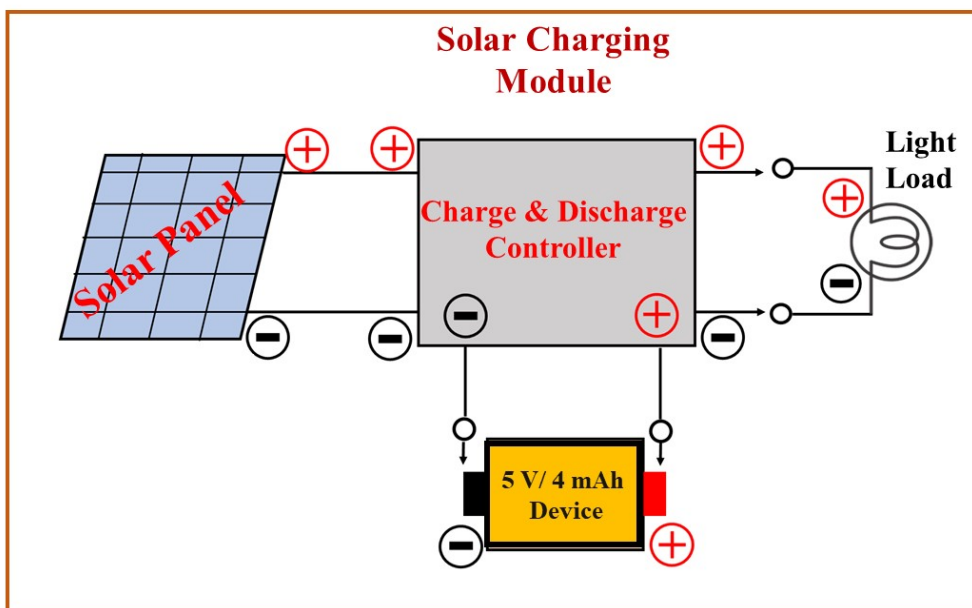


Figure S10: Schematic representation of customs-built solar-charging cum LED-discharging module for prototype battery testing.

References

- S1. Y. Zhang, Z. Su and J. Ding, Synthesis and electrochemical properties of Ge-doped $\text{Li}_3\text{V}_2(\text{PO}_4)_3/\text{C}$ cathode materials for lithium-ion batteries. *J. Alloys Compd.*, 2017, **702**, 427-431.
- S2. C. Liu, Z. Neale, J. Zheng, X. Jia, J. Huang, M. Yan, M. Tian, M. Wang, J. Yang and G. Cao, Expanded hydrated vanadate for high-performance aqueous zinc-ion batteries. *Energy & Environmental Science*, 2019, **12**, 2273-2285.